Photoactivity of Nano-oxide Layers of Screen Printed DSSC on Glass and PET Foils

Milan Mikula, Pavol Gemeiner, Vladimír Dvonka, Peter Gabovič
Department of Printing Arts Technology and Photochemistry IPM, Faculty of Chemical and Food Technology SUT in Bratislava

Abstract: Polyethylene-terephthalate (PET) foils and glass slides coated with thin conductive layers were used as substrates for TiO_2 or ZnO based photoactive electrodes of dye-sensitized solar cells (DSSC). The nanoparticle oxides were applied onto the substrates in a form of alcohol pastes by screen printing or by doctor blade technique. Photocurrents and I-V load characteristics were measured depending on the solar cell composition and preparation. The influence of thin TiO_2 blocking layer prepared by sol-gel technique is discussed.

Keywords: TiO_2, ZnO, solar cell, PET, screen printing

Introduction

PET foil is a promising support and encapsulating material in organic and printed electronics, including photovoltaic applications. In the case of Dye Sensitized Solar Cells (DSSC) the standard photoactive layers based usually on TiO_2 nanoparticles on glass substrates involve sintering at 450°C. In order to prepare a flexible solar cell on polymer plastic substrates (PET, PEN,...) low temperature processes (below 150°C) of the coating of all functional layers ought to be discovered. To keep a low cost production the roll-to-roll processes are preferred, including screen printing, knife over edge (doctor blade), slot die and all printing techniques [1,2].

The nano and microstructure of the active oxide layer (TiO_2) is critical to DSSC performance. In a low T curing process, TiO_2 film has the tendency to crack, resulting in the shunt of the device and reduction of solar cell efficiency. An alternative ZnO films have better morphology tolerance and mostly the interparticle contacts keep uninterupted [3].

To prevent the internal shortening of the cells fabricated from a binder-free nanoparticle-oxide pastes at low T a thin blocking layer, usually of an amorphous TiO_2, is deposited onto the substrate (ITO/PET) before photoactive oxide layer deposition. This hole blocking layer (BL) also avoids direct contact of the dye with the ITO surface. The electron conductive BL can be created chemically [4], physically by atomic layer deposition [5] or by sol-gel (SG) process [6].

The SG process is based on hydrolysis and polycondensation of titania alcoxides, creating the oxide network in a gel form. After solvent evaporation the xerogel is built and calcination step above 300°C is used to make it denser, ideally of anatase structure for application in photocatalysis or photovoltaics. To keep the low T technology, recently plasma treatments have been used as a calcination step for removal of organic additives and generation of mesoporous films with sol–gel precursors [7].

In this paper, physical and photoelectric properties of printed photoactive oxide layers and DSSC (finalized using standard iodine electrolyte and counter electrode of Pt) on PET and glass substrates with the co-deposited BL layers were measured and correlated with overall cell structure and UV/plasma pretreatment of BLs. The solar cells were characterized measuring the photocurrent Iph and cell voltage U depending on the circuit loading (I-V loading curve [1]) under the standard day-light (1sun) illumination.

Experimental

Two electrically conductive substrates (Aldrich), PET foils (120μm) and glass slides (2 mm) coated by thin indium oxide layer (ITO, 100 Ω/sq.) or fluorine dopped oxide (FTO, 7 Ω/sq.), resp., were coated by nanoparticle metal oxides TiO_2 (20 nm, Degussa P25, Evonik) or ZnO (<100 nm, Aldrich) and used as bases for solar cell (dye-sensitized, DSSC) preparation.

Two different types of nanopastes were prepared for both oxides. One, standard type for the screen printing application onto a glass substrates including sintering at 450°C (metal-oxide, ethanol, water, acetylic acid, ethylcellulose [8]) and another paste type for low temperature application onto the plastic substrates (PET, with the curing temperature below 130°C). In the latter case the powder nano-oxides were first homogenized in butanol (oxide/butanol = 2/5) first manually and then in agate ball mill (2 hours). In some cases the nano-oxide was mixed (1:1) with the more rough oxide (170 nm anatase-TiO_2 or ~200 nm ZnO).

The prepared standard pastes were applied by screen printing onto the FTO-glass and sintered (450°C, 30 min., resulting in thickness of 1.5 μm). Low temperature pastes were applied onto ITO/PET substrates (clean and UV treated) by doctor blade in thickness of about 50 μm and cured 30 min at 120°C in air, or at 90°C in vacuum (resulting in 15 μm). The standard Ru-dye (N3, Aldrich) was adsorbed into the cured mesoporous oxide layers from dye-ethanol solution (0.4 mM).

To prevent the internal short currents [1,3] of final solar cells, onto some substrates the very thin blocking (barrier) layer was deposited before oxide layers application described above. The blocking layers were deposited by sol-gel technique, e.g. by the simple dip coating applying the sol of 1% TiO_2 (Ti-tetrabutoxide in ethanol, stabilized by HNO_3, the draw up rate was 10 cm/min) [6]. To increase the electric conductivity without sintering, the sol-gel (SG) layers were treated by UV light (250 W Hg lamp) or by dielectric barrier discharge plasma (10 kHz, 2W/cm²) at atmospheric pressure in air.
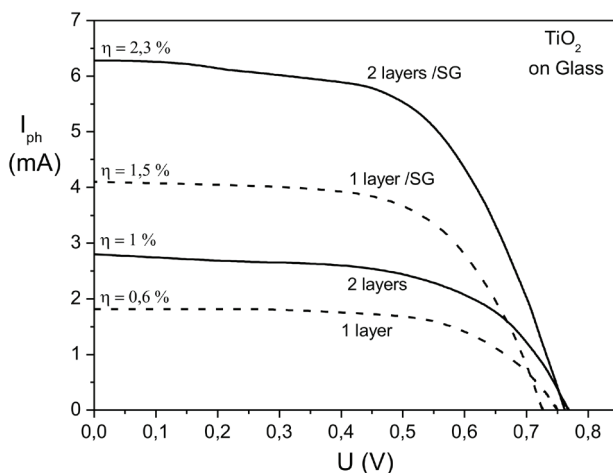

Figure 1: I-V loading curves of standard screen printed TiO_2 DSSC on FTO glass. (2 layers denotes 2 times screen printed of nanopaste, and SG denotes sol-gel blocking layer)

The solar cells were finalized by contacting (face to face) the prepared oxide electrode (on PET or on glass) and the Pt counterelectrode on FTO/glass substrate, after dropping an iodine electrolyte into the oxide layer between. (Pt layer was created by doctor blading of nano-Pt paste, Solaronix, and sintering at 450°C. In some experiments the Pt layers were replaced by commercial conductive polymer PEDOT:PSS). The active area of the cells was around 1.5 cm².

Afterwards, the solar cells were characterized measuring the photocurrent and cell voltage depending on the circuit loading (I-V loading curve [1]) under near the standard day-light illumination (880 W/m^2, metal halide lamp box) by multimeters Keithley 2000 and Metex M-3650D. UV-Vis. absorption and AC conductivities (10 kHz) of sol-gel layers were measured by spectrometer CECIL 3055 and by LCR Digibridge Quadtech 1715, respectively. The surface nano-texture of the layers was studied by atomic force microscopy, Veeco, CP II.

Results and discussion

The photocurrent – voltage dependence of the standard composition of screen printed DSSC (sintered TiO_2 on FTO-glass, Fig. 1) had a standard shape and the photocurrent was significantly increased after incorporating the sol-gel layer (SG, more than 2 times) and with the oxide thickness.

However, when applying the oxide layers onto PET substrates (with free drying), the photocurrents strongly decrease due to the worse contacts between non-sintered nanoparticles and more due to the low conductivity of non-sintered sol-gel layers. The thickness and the specific resistivity of the coated non-treated SG layers were 20 nm and round 20 kΩm, resp. (The specific resistivity of the crystalline anatase phase of TiO_2 is referred to round 0.1 Ωm.) So the series resistivity of active area (1.5 cm^2) of the SG layer as electrode was just 3 Ω. Consequently, supposing the better interparticle contacts and lower sensitivity to thermal treatment of ZnO systems [3] the ZnO pastes were dominantly applied onto PET, without and including TiO_2 sol-gel blocking layer (Fig. 2).
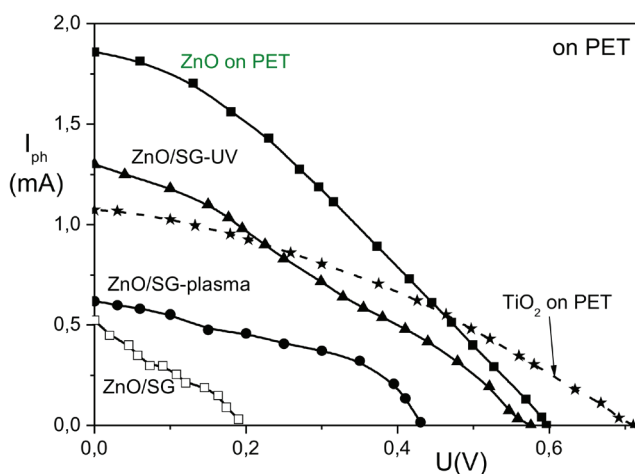

Figure 2: I-V curves of low temperature ZnO DSSC on PET substrates (TiO_2 for comparison). SG denotes the presence of sol-gel layer, plasma and UV the manner of the SG layers treatment.

The plasma (20 sec.) or UV treatment (10 min.) of the SG layers had very non-reproducible effect on the solar cell performance (the best cases are in Fig. 2), while the resistivity of the treated layers decreased just to 85% and 75% of the nontreated values, respectively. The absorption of SG layers in UV-C region (Fig. 3) is very high, so some reconstruction of the amorphous free volume rich SG layers can occur after strong UV exposition.

There is a chance that in the case of thinner and compact SG layers the photocurrent would increase. The compactness and the texture on nano-level can be seen in AFM images (Fig. 4). The root mean square roughness of the base ITO layer (1.3 nm) is similar to that of SG layers (1.1

nm), but the texture is different. Above the microscale, the prepared xerogel layers were free of cracks and precipitates.
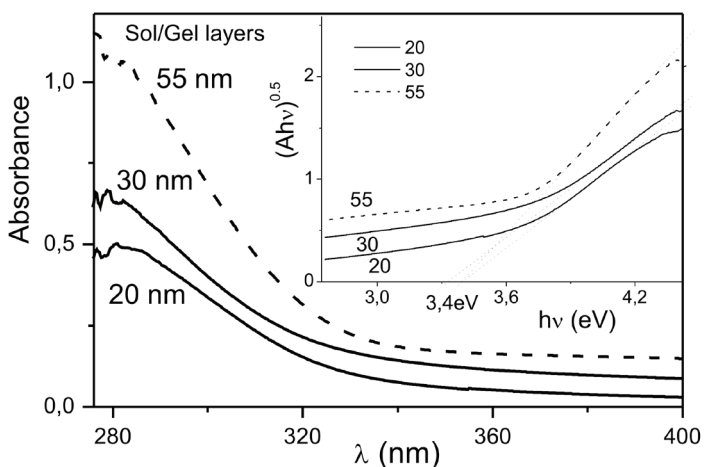

Figure 3: Absorption spectra and optical gap (inlet) of sol-gel layers with different thickness. The gap is higher than that of anatase (3.2 eV). The thinnest (20 nm) SG layer was chosen for all experiments above.
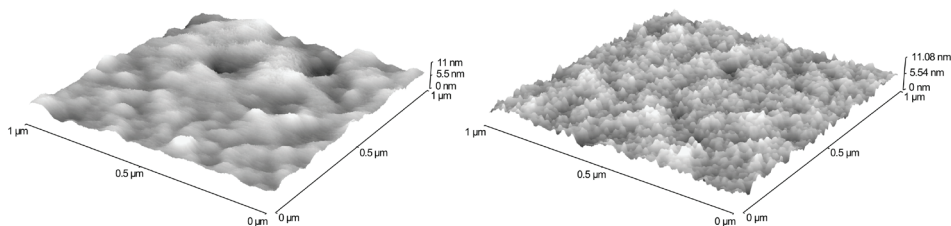

Figure 4: Surface topography of ITO and sol-gel/ ITO layers on PET. (AFM microscopy, tapping mode)

The inclined shape of I-V characteristic (Fig. 2) was similar for all ZnO and TiO_2 cells on PET substrates and different comparing with standard sintered cells on glass (Fig. 1). Very inclined slope decreases significantly the solar cell efficiency, so it is important to get the sharp slope at the open circuit position. The slope is connected with the internal series resistance of a cell, e.g. it correlates with the interparticle contacts (sharp slope = good contact = low series resistance).

To improve the interparticle contacts of our oxide particles the layers were pressured (~10N/ cm^2) during the drying process at higher temperatures (90 and 130°C). The slopes and the photocurrents had increased with the application of pressure and temperature (Fig. 5), as well as with the homogenization of the oxide pastes in ball mill.

Afterwards, the rough and fine-grained oxides were combined to improve the oxide layer structure and SC performance (Fig. 6). Despite the higher photocurrents in ZnO case, the slope is still too inclined (too high internal resistance). Used ITO layer on the PET foil has much higher resistance (100 Ω/sq.) than FTO on the glass (7 Ω/sq.). To taste the influence of ITO resistance to overall series resistance (and to solar cell efficiency) the ZnO layer (the best combination)

was applied also onto the FTO glass by the same low temperature process as onto the PET foils (without sintering). The dash curve in Fig. 6 confirms the strong effect of ITO resistance. The whole shape of the ZnO curve on FTO substrate is illustrated in Fig. 7, including the results of solar cells composition with PEDOT counter elctrodes, as an alternative of Pt layers.
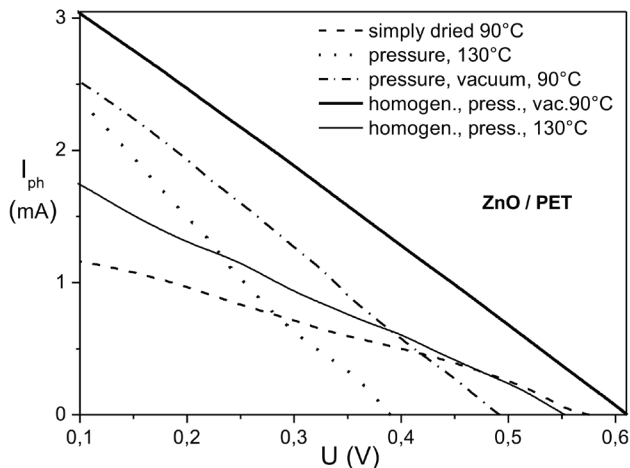
Figure 5: I-V loading curves for ZnO system on PET at different photolayer preparation (simply doctor bladed, applied pressure during drying, homogenization in vibration ball mill,...).
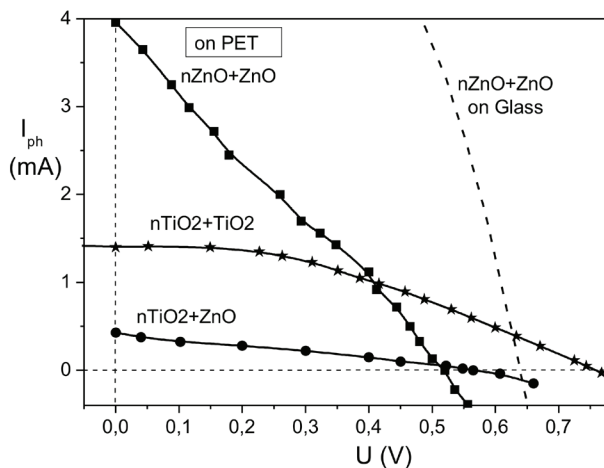
Figure 6: I-V loading curves for ZnO system on PET in different combination of fine nano-oxides with more rough oxides (homogenization in ball mill).

Conclusions

Mesoporous TiO_2 and ZnO photoactive electrodes of DSSC solar cells were prepared on PET and glass substrates by screen printing and doctor blade technique. Considerable enhancement of solar cell efficiency by sol gel blocking sublayer found in the case of sintered oxide photolayers on glass did not occur in the case of low temperature process on PET substrates. The better performance of ZnO layers in comparison with TiO_2 ones on PET foils was confirmed. Different

preparation of photoactive oxides gave very different photocurrent response with relative high internal resistance of the oxide and of the other layers too (including ITO layer). Next work flow optimalization is necessary.
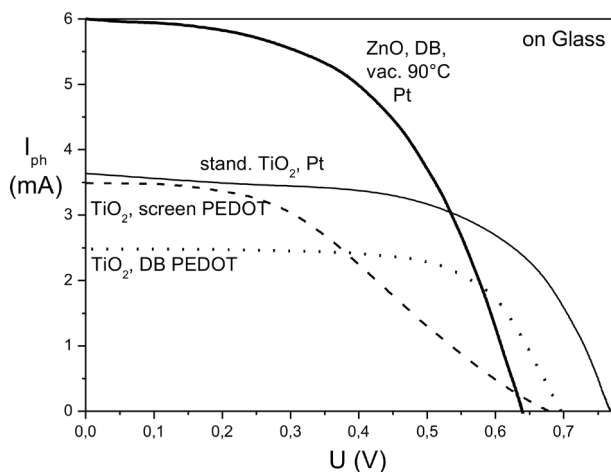

Figure 7: I-V loading curves for different systems on glass with PEDOT and Pt as counterelectrode

Acknowledgement

References

1. Pagliaro M., Palmisano G., Ciriminna R.: Flexible solar cells, Wiley-VCH, Weinheim, 2008.
2. Wei D.: Dye sensitized solar cells, Int. J. Mol. Sci. *11*, 1103 (2010).
3. Wang B., Kerr L.L.: Solar Energy Materials and Solar Cells *95*, 2531 (2011).
4. Mane R.S., Lee W.J., Pathan H.M., Han S.H.: J. Phys. Chem. B *109*, 24254 (2005).
5. Jiang C.Y., Koh W.L., Leung M.Y. et al.: Appl. Phys. Lett. *100*, 113901 (2012).
6. Šandrej M., Mikula M., Gemeiner P.: Chem. Listy *105*, s334 (2011).
7. Huang J., Ichinose I., Kunitake T., Nakao A.: Langmuir *18*, 9048 (2002).
8. Fan K., Liu M., Peng T., Ma L., Dai K.: Renewable Energy, *35*, 555 (2010).